

## Microstructures and mechanical properties of Mg-10Ho-0.6Zr- $x$ Nd alloys

LIU Bao-zhong(刘宝忠)<sup>1</sup>, LIU Jiao-jiao(刘娇娇)<sup>1</sup>, HOU Xiu-li(侯秀丽)<sup>2,3</sup>,  
ZHANG Zhi(张志)<sup>1</sup>, LI Lei(李雷)<sup>1</sup>, WANG Li-min(王立民)<sup>3</sup>

1. School of Materials Science and Engineering, Henan Polytechnic University, Jiaozuo 454000, China;
2. Key Laboratory of Automobile Materials, Ministry of Education, Jilin University, Changchun 130025, China;
3. State Key Laboratory of Rare Earth Resource Utilization, Changchun Institute of Applied Chemistry, Chinese Academy of Sciences, Changchun 130022, China

Received 23 September 2009; accepted 30 January 2010

**Abstract:** Mg-10Ho-0.6Zr- $x$ Nd ( $x=0, 1, 3$  and  $5$ , mass fraction, %) alloys were prepared by metal mould casting, and the microstructures and mechanical properties were investigated. The results show that the grain size of as-cast alloys reduces and the hardness and strength increase with the increase of Nd content. The alloys are aged followed by solid solution treatment. Mg-10Ho-0.6Zr-3Nd and Mg-10Ho-0.6Zr-5Nd alloys exhibit obvious age hardening response. The hardness value of Mg-10Ho-0.6Zr-5Nd alloy increases from HV104 at as-cast state to HV136 at peak-aged state. The maximum ultimate tensile strength and yield strength of the Mg-10Ho-0.6Zr-5Nd alloy are obtained in at peak-aged state, and the values are 323 MPa, 212 MPa at room temperature, and 258 MPa, 176 MPa at 250 °C, respectively. The improvement of the tensile strength is mainly attributed to the fine and dispersively distributed plate-shaped  $\beta'$  metastable phase.

**Key words:** Mg-Ho-Zr-Nd alloy; microstructure; age hardening behavior; mechanical properties

## 1 Introduction

In the past decade, there has been a significant growth in the research of high strength, light-weight magnesium alloys for elevated temperature applications. Magnesium alloys containing rare earth (RE) elements have become the focus of the investigations. The Mg-HRE (heavy rare earth) alloys exhibit remarkable solution strengthening and age-hardening response after heat processing due to its large solubility of HRE in Mg at high temperature and obvious decrease with decreasing temperature. Thus, many fundamental researches in developing new Mg alloys containing HRE elements have been carried out[1-8]. Rare earth element holmium (Ho) is an important element of heavy rare earth elements. The chemical property of Ho is similar to that of Gd and Y. Recently, it has been reported that Ho additions could effectively improve the heat resistance of Mg alloys because of the formation of metastable and stable precipitates in the alloys. It is very promising to develop new heat resistance Mg-Ho based alloys by suitable heat treatment. Some investigations about

microstructures, age hardening response and mechanical properties of Mg-Ho-Y alloys have been done[7]. The alloys exhibit high ultimate tensile strength, yield strength and ductility. It is known that the binary Mg-Gd alloys containing less than 10%Gd show little or no precipitation hardening response during isothermal or isochronal ageing of supersaturated solid[8]. Accordingly, it is possible that binary Mg-Ho alloys containing low Ho show little or no precipitation hardening response during isothermal or isochronal ageing. However, high Ho content causes the increase of cost and the decrease of elongation. Thus, it is necessary to add a little of other elements to substitute part of Ho to reduce the cost without purifying process and enhance mechanical properties.

ROKHLIN et al[9] reported that Mg alloys containing two kinds of rare-earth elements belonging to different subgroups can promote strengthening effectively. Mg-8Gd-0.6Zr- $x$ Nd alloys show that the addition of Nd can improve the hardness and the age hardening behavior significantly, which is contributed to  $\beta'$ -Mg<sub>12</sub>RE and  $\beta$ -Mg<sub>5</sub>RE precipitates[10]. A four-stage precipitation sequence of Mg-11Gd-2Nd-0.5Zr (mass

fraction, %) alloy aged at 250 °C can be described as follows: supersaturated  $\alpha$ -Mg solid solution  $\rightarrow$   $\beta''$ (DO19)  $\rightarrow$   $\beta'$ (cubo)  $\rightarrow$   $\beta_1$ (fcc)  $\rightarrow$   $\beta$ (fcc), where the later precipitate can coexist with the former[11]. While, the element of Nd can also increase the yield strength in Mg-8Gd-0.6Zr- $x$ Y- $y$ Nd ( $x+y=3$ ) alloys[12]. Up to date, few investigations have been done on the Mg-Ho based alloys with the addition of other rare earth elements. In this work, the effects of Nd on the microstructures, age hardening response and mechanical properties of Mg-10Ho-0.6Zr- $x$ Nd ( $x=0, 1, 3$  and  $5$ , mass fraction, %) alloys were investigated.

## 2 Experimental

The alloys with nominal compositions of Mg-10Ho-0.6Zr (A), Mg-10Ho-0.6Zr-1Nd (B), Mg-10Ho-0.6Zr-3Nd (C) and Mg-10Ho-0.6Zr-5Nd (D) were prepared by melting in an electric resistance furnace in the graphite crucible under an anti-oxidizing flux. The elements of Ho, Nd and Zr were added in the form of Mg-20Ho, Mg-20Nd and Mg-30Zr master alloys (mass fraction, %), respectively. After the elements were entirely dissolved and homogenized at 770 °C for 30 min, the melt was cast into a preheated copper mould at 720

. The dimensions of the castings are 70 mm×40 mm×13 mm. The actual chemical composition of the ingots were presented in Table 1, which was analyzed by inductively coupled plasma (ICP). Specimens cut from the as-cast ingots were first solution treated at 530 °C for

8 h, and then quenched into water at about 60 °C, finally aged at 230 °C. The microstructures were observed by optical microscope (OM) after polishing and etching. Phase structure and morphology were characterized by X-ray diffractometer (XRD) and transmission electron microscope (TEM). Microhardness testing was taken with 0.25 N load and holding time 15 s by FM-100 Vickers microhardness tester. Tensile testing was performed on a standard test machine at room temperature (RT) and 250 °C with a strain rate of 1 mm/min. As for elevated temperature tensile test, the samples were soaked for 10 min at the test temperature before loading.

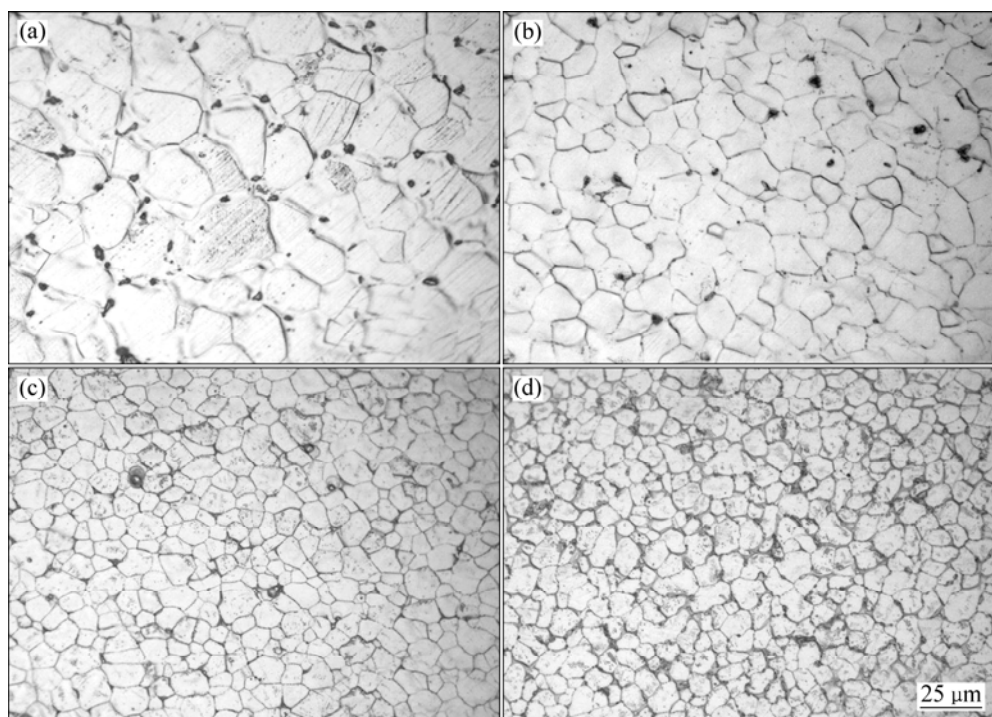
**Table 1** Chemical composition of Mg-10Ho-0.6Zr- $x$ Nd alloys (mass fraction, %)

Alloy	Ho	Zr	Nd	Mg
A	9.10	0.530	0	Bal.
B	9.33	0.539	1.13	Bal.
C	8.88	0.460	3.14	Bal.
D	8.74	0.429	5.47	Bal.

## 3 Results and discussion

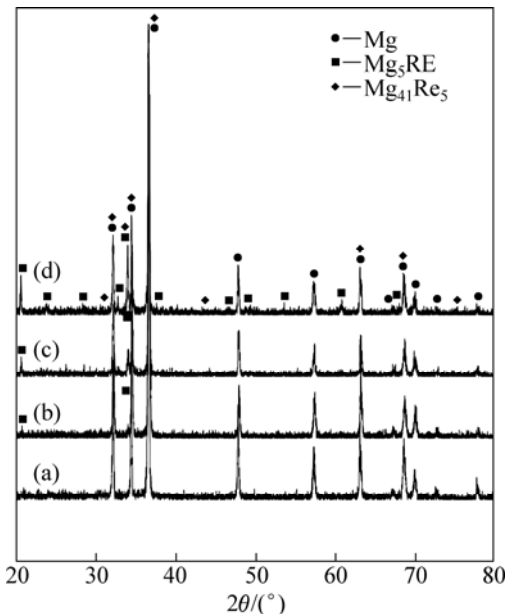
### 3.1 Microstructures

Fig.1 shows the microstructures of the as-cast Mg-10Ho-0.6Zr- $x$ Nd alloys. The alloys are mainly comprised of  $\alpha$ -Mg matrix and network grain boundaries. Some dispersed precipitates can be observed in the



**Fig.1** Microstructures of as-cast Mg-10Ho-0.6Zr- $x$ Nd alloys: (a)  $x=0$ ; (b)  $x=1$ ; (c)  $x=3$ ; (d)  $x=5$

alloys, and the amount of precipitates increases with increasing Nd content. The average grain sizes of alloys A, B, C and D are about 37, 21, 15, 13  $\mu\text{m}$ , respectively. XRD results of the as-cast alloys are shown in Fig.2. It indicates that alloy A consists of  $\alpha$ -Mg solid solution. Alloys B and C are composed of  $\alpha$ -Mg solid solution and a small amount of  $\text{Mg}_5(\text{Nd}, \text{Ho})$  phase.  $\text{Mg}_{41}(\text{Nd}, \text{Ho})_5$  phase is observed in alloy D with the exception of  $\alpha$ -Mg and a lot of  $\text{Mg}_5(\text{Nd}, \text{Ho})$  phase.



**Fig.2** X-ray diffraction patterns of as-cast Mg-10Ho-0.6Zr-xNd alloys: (a)  $x=0$ ; (b)  $x=1$ ; (c)  $x=3$ ; (d)  $x=5$

The microstructures of the aged Mg-10Ho-0.6Zr-xNd alloys are shown in Fig.3. It indicates that alloys A, B and C are mainly composed of  $\alpha$ -Mg matrix and fine network grain boundaries. Furthermore, some dispersed precipitates are observed in the matrix. Especially, alloy D shows a phenomenon of some small Zr-containing particles precipitated at grain interior, and some Nd-rich second phases precipitated at grain boundaries and the triple grain junctions. The similar phenomena are also observed in Mg-3Nd-0.2Zn-0.4Zr alloy[13]. In addition, the aged alloy D obtains the smallest grain size (about 25  $\mu\text{m}$ ). Fig.4 shows XRD results of the aged alloys at peak hardness. It demonstrates that alloys A, B and C are mainly composed of  $\alpha$ -Mg solid solution. Alloy D consists of  $\alpha$ -Mg and a small quantity of  $\text{Mg}_{41}(\text{Ho}, \text{Nd})_5$ .  $\text{Mg}_5(\text{Nd}, \text{Ho})$  phase cannot be observed. However, the metastable phase formed during the aging process is hardly detected because of the small volume fraction and the limited particle size. It should be point out that the above results are obtained based on TEM analysis to be presented later.

### 3.2 Age hardening behavior

Fig.5 shows the age hardening behavior of the alloys aged at 230  $^{\circ}\text{C}$ . It is observed that alloys A and B exhibit weak hardening response during isothermal aging, while alloys C and D exhibit obvious age hardening response. The water-quenched hardness (QHV) of alloy C is HV96, and then reach to the peak hardness (PHV) of HV122 after aging for 24 h. A more significant increase

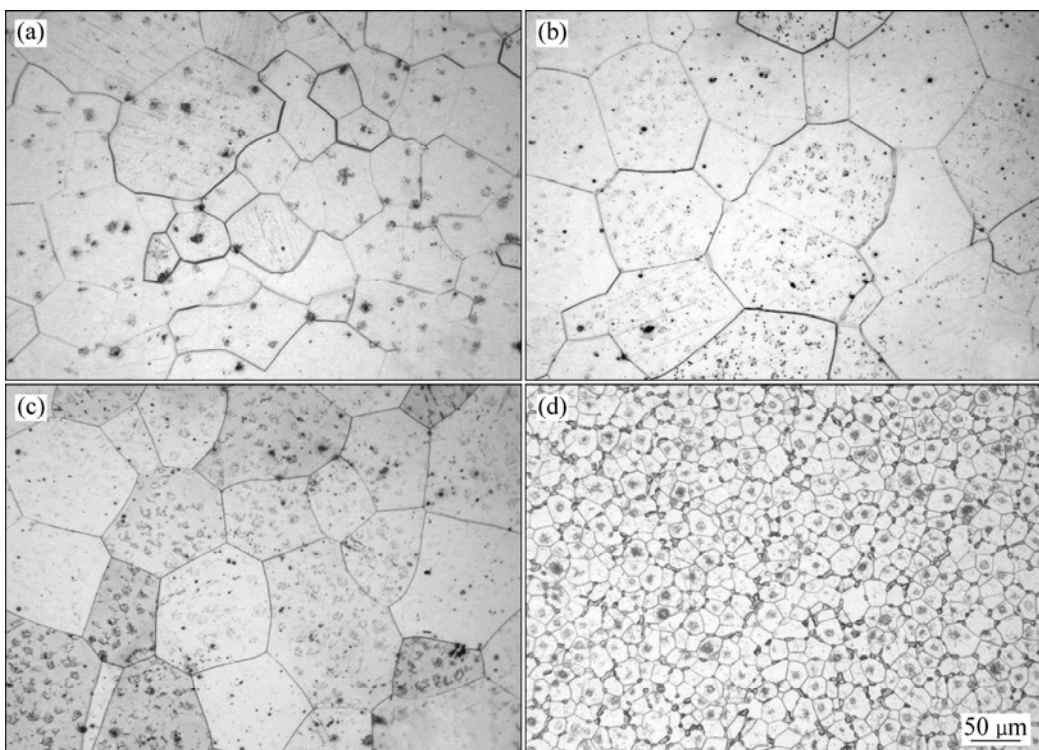


**Fig.3** Microstructures of Mg-10Ho-0.6Zr-xNd alloys at peak hardness: (a)  $x=0$ ; (b)  $x=1$ ; (c)  $x=3$ ; (d)  $x=5$

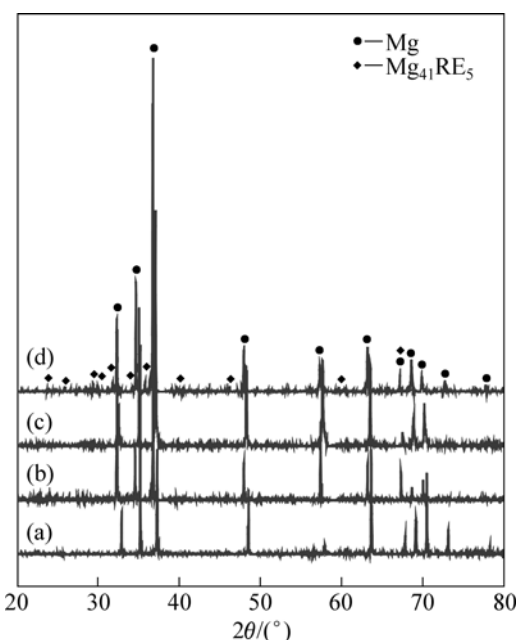


**Fig.4** X-ray diffraction patterns of aged Mg-10Ho-xNd-0.6Zr-xNd alloys at peak hardness: (a)  $x=0$ ; (b)  $x=1$ ; (c)  $x=3$ ; (d)  $x=5$

in QHV and PHV of alloy D can be observed compared with alloy C. The peak hardness is obtained after aging for 16 h and the value increases from 101 at water-quenched state to 136 at peak-aged state. After reaching the PHV, the hardness remains stable over a relatively long heating time and then gradually decreases as a result of over-aging. Fig.6(a) shows TEM image of peak-aged alloy D and electron diffraction (SAED) pattern of corresponding selected area with the electron beam parallel to  $[2\bar{1}\bar{1}0]_{\alpha}$  is shown in Fig.6(b). A large amount of fine plate-like precipitates are observed in alloy D and the size of the precipitates is about 20 nm. This similar precipitate is also reported in the previous literature[14]. Generally, Mg-RE alloy systems exhibit a four-staged precipitation sequence involving S.S.S.S. (cph)  $\rightarrow$   $\beta''$ (DO19)  $\rightarrow$   $\beta'$ (cbco)  $\rightarrow$   $\beta_1$ (fcc)  $\rightarrow$   $\beta$ (fcc), which has been observed in Mg-Gd-Nd[11] as well as Mg-Y-Nd[15–16] alloys. At the early stage, the hardness increases slightly due to the precipitation of  $\beta''$ -phase, but  $\beta''$ -phase disappears quickly in the very early stage. Then the formation of  $\beta'$  metastable phase makes the hardness increase quickly and plays a dominant role in the age hardening process. So, we can say that  $\beta'$ -phase, which has a base centered orthorhombic structure ( $a=0.640$  nm,  $b=2.223$  nm,  $c=0.521$  nm) contributes to the age hardening behavior. The orientation relationship of the  $\beta'$  precipitates and  $\alpha$ -Mg matrix is  $[001]_{\beta'}//[0001]_{\alpha}$  and  $(100)_{\beta'}//(2\bar{1}\bar{1}0)_{\alpha}$ . With prolonging aging time, the coarse  $\beta_1$  and  $\beta$  phases make the hardness decline. However, the strengthening factors are more complicated in ternary Mg-RE alloys. It has been reported that

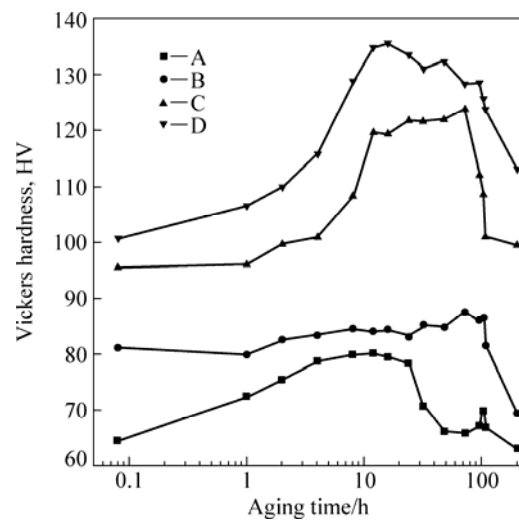


**Fig.5** Aging curves of Mg-10Ho-xNd-0.6Zr alloys

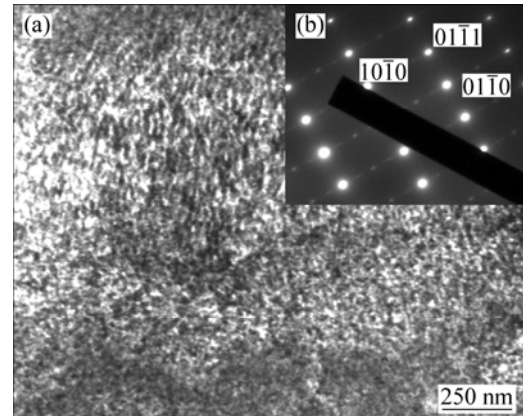


**Fig.6** TEM image (a) and corresponding SAED pattern (b) in peak-aged alloy D ( $B//[2\bar{1}\bar{1}0]_{\alpha}$ )

$\beta'$ -Mg<sub>12</sub>NdY and  $\beta$ -Mg<sub>14</sub>Nd<sub>2</sub>Y contributed to precipitation strengthening in alloys WE54 and WE43[15–16]. Thus, the strengthening mechanism of alloy D is similar to that observed in alloys WE54 and WE43.

Furthermore, the ageing curves indicate that increasing Nd content is beneficial to QHV and PHV of the investigated alloys, which can be ascribed to the following factors. Firstly, the eutectic phase dissolves into the matrix and the alloying elements Ho and Nd homogenously distribute through out the grains after solution. The increase of PHV is mainly attributed to precipitation hardening. Secondly, the solubility of Ho in  $\alpha$ -Mg matrix is reduced relatively with increasing Nd content. As a result,  $\beta'$  precipitation containing Ho concentrates and reaches the PHV.

### 3.3 Mechanical properties

The mechanical properties including room temperature (RT) Vickers hardness (HV), ultimate tensile

strength (UTS), yield strength (YS) and elongation ( $\delta$ ) of the as-cast alloys are shown in Table 2. As-cast alloys exhibit similar mechanical properties at room temperature and 250 °C. By adding Nd, HV of the alloys appreciably increases as UTS and YS of the alloy do, while the tensile elongation decreases at RT but increases at 250 °C. Alloy D exhibits the highest HV, UTS and YS. At RT, the values are HV104, 239 MPa and 166 MPa, respectively. At 250 °C UTS and YS are 206 MPa and 122 MPa, respectively. The corresponding mechanical properties of the alloys at peak hardness are listed in Table 3. The trend of the results is similar to that at the as-cast state but the values of HV, UTS and YS obviously increase. The maximum UTS and YS are obtained in alloy D peak-aged at 230 °C for 16 h, and the values are 323 MPa and 212 MPa respectively at RT, 258 MPa and 176 MPa at 250 °C, respectively. These values are about 2 times those of alloy A. The elongation greatly reduces from 15.9% at as-cast station to 3.6% at peak-aged state at 250 °C.

**Table 2** Tensile properties of Mg-10Ho-0.6Zr-xNd as-cast alloys

Alloy	HV	UTS/MPa		YS/MPa		$\delta$ /%	
		RT	250 °C	RT	250 °C	RT	250 °C
A	67	183	120	83	61	10.8	11.7
B	83	186	136	106	89	6.9	7.0
C	97	228	200	140	108	6.6	13.9
D	104	239	206	166	122	3.9	15.9

**Table 3** Tensile properties of Mg-10Ho-0.6Zr-xNd alloys at peak-aged state

Alloy	HV	UTS/MPa		YS/MPa		$\delta$ /%	
		RT	250 °C	RT	250 °C	RT	250 °C
A	80	184	133	92	71	8.6	11.7
B	87	191	175	116	100	5.5	9.0
C	122	240	230	156	170	3.6	4.0
D	136	323	258	212	176	3.2	3.6

In light of the above precipitation sequence and mechanical properties results, it is found that  $\beta''$  phase should be the key strengthening phase in the alloy. The nucleation of  $\beta''$  causes the rapid age-hardening response at the early stage of aging, and the peak strength is encountered corresponding to a critical dispersion of  $\beta''$  precipitates. In addition, the added Nd element itself has a significant age hardening due to the very little solid solubility in Mg. Furthermore, the average grain size of aged Mg-10Ho-0.6Zr-5Nd alloy is very smaller compared with other alloys. This is a very important

factor for the highest mechanical properties.

## 4 Conclusions

1) The microstructure and mechanical properties of as-cast and aged Mg-10Ho-0.6Zr-xNd alloys were investigated. The as-cast alloys consist of  $\alpha$ -Mg, Mg<sub>5</sub>(Nd, Ho) phase and Mg<sub>41</sub>(Nd, Ho)<sub>5</sub> phase. By increasing Nd content, the size of as-cast alloys decrease. After the alloys are aged followed by solid solution treatment, Mg<sub>5</sub>(Nd, Ho) phase generally disappears and a large amount of fine plate-like precipitates are observed in the alloys.

2) The alloys Mg-10Ho-0.6Zr-3Nd and Mg-10Ho-0.6Zr-5Nd exhibit obvious age hardening response,  $\beta''$  phase should be the key strengthening phase in the alloy, and the hardness increases from HV104 at as-cast state to HV136 at peak-aged state.

3) The maximum ultimate tensile strength and yield strength are obtained in Mg-10Ho-0.6Zr-5Nd alloy at peak-aged state, and the values are 323 MPa, 212 MPa at room temperature respectively, and 258 MPa, 176 MPa at 250 °C respectively. The improvement of the mechanical properties of aged alloy D is attributed to the fine and dispersively  $\beta''$  precipitates.

## References

- [1] BETTLES C J, GIBSON M A. Microstructural design for enhanced elevated temperature properties in sand-castable magnesium alloys [J]. Advanced Engineering Materials, 2003, 5(12): 859–865.
- [2] LI Da-quan, WANG Qu-dong, DING Wen-jiang. Effect of heat treatments on microstructure and mechanical properties of Mg-4Y-4Sm-0.5Zr alloy [J]. Materials Science and Engineering A, 2007, 448: 165–170.
- [3] LI Da-quan, WANG Qu-dong, DING Wen-jiang. Characterization of phases in Mg-4Y-4Sm-0.5Zr alloy [J]. Materials Science and Engineering A, 2006, 428: 295–300.
- [4] LIU Ke, ZHANG Jing-huai, ROKHLIN L L, ELKIN F M, TANG Ding-xiang, MENG Jian. Microstructures and mechanical properties of extruded Mg-8Gd-0.4Zr alloys containing Zn [J]. Materials Science and Engineering A, 2009, 505: 13–19.
- [5] LI De-hui, DONG Jie, ZENG Xiao-qin, LU Chen, DING Wen-jiang. Characterization of precipitate phases in a Mg-Dy-Gd-Nd alloy [J]. Journal of Alloys and Compounds, 2007, 439: 254–257.
- [6] LI De-hui, DONG Jie, ZENG Xiao-qin, LU Chen, DING Wen-jiang. Characterization of  $\beta''$  precipitate phase in a Mg-Dy-Gd-Nd alloy [J]. Materials Characterization, 2007, 58: 1025–1028.
- [7] WANG Jun, ZHANG De-ping, MENG Jian. Effect of Y for enhanced age hardening response and mechanical properties of Mg-Ho-Y-Zr alloys [J]. Journal of Alloys and Compounds, 2008, 454: 194–200.
- [8] VOSTRÝ P, STULÍKOVÁ I, SMOLA B, VON BUCH F, MORDIKE B L. Microstructure evolution in isochronally heat treated Mg-Gd alloys [J]. Phys Status Solidi A: Appl Res, 1999, 175: 491–500.

[9] ROKHLIN L L, DOBATKINA T V, NIKITINA N I. Constitution and properties of the ternary magnesium alloys containing two rare-earth metals of different subgroups [J]. Materials Science Forum, 2003, 419/422: 291-296.

[10] PENG Qiu-ming, WU Yao-ming, FANG Da-qing, MENG Jian, WANG Li-min. Microstructures and mechanical properties of Mg-8Gd-0.6Zr-xNd ( $x=0,1,3,5$ ) alloys [J]. *J Mater Sci*, 2007, 42: 3908-3913.

[11] ZHENG Kai-yun, DONG Jie, ZENG Xiao-qin, DING Wen-jiang. Precipitation and its effect on the mechanical properties of a cast Mg-Gd-Nd-Zr alloy [J]. Materials Science and Engineering A, 2008, 489: 44-54.

[12] PENG Qiu-ming, WANG Jian-li, WU Yao-ming, WANG Li-min. Microstructures and tensile properties of Mg-8Gd-0.6Zr-xNd-yY ( $x+y=3\%$ ) alloys [J]. Materials Science and Engineering A, 2006, 433: 133-138.

[13] FU Peng-huai, PENG Li-ming, JIANG Hai-yan, CHANG Jian-wei, ZHAI Chun-quan. Effect of heat treatments on the microstructures and mechanical properties of Mg-3Nd-0.2Zn-0.4Zr(wt %) alloy [J]. Materials Science and Engineering A, 2008, 486: 183-192.

[14] ANYANWU I A, KAMADO S, KOJIMA Y. Aging characteristics and high temperature tensile properties of Mg-Gd-Y-Zr alloys [J]. *Mater Trans*, 2001, 42: 1206-1211.

[15] NIE J F, MUDDLE B C. Characterisation of strengthening precipitate phases in a Mg-Y-Nd alloy [J]. *Acta Materialia*, 2000, 48: 1691-1703.

[16] ANTION C, DONNADIEU P, PERRARD F, DESCHAMPS A, TASSIN C, PISCH A. Hardening precipitation in a Mg-4Y-3RE alloy [J]. *Acta Materialia*, 2003, 51: 5335-5348.

(Edited by CHEN Ai-hua)